International Journal of Automation, Mechatronics & Robotics
Volume 3 : Issue 1 [ISSN 2374-1546]
Publication Date : 31 August, 2016

Schlieren Visualization of Water Natural Convection in a Vertical Ribbed Channel

Marco Fossa, Mario Misale, Giovanni Tanda

***Abstract*—Schlieren techniques are valuable tools for the qualitative and quantitative visualizations of flows in a wide range of scientific and engineering disciplines. In this work, a schlieren technique is applied to visualize the buoyancy-induced flow inside vertical ribbed channels using water as convective fluid. The test section consists of a vertical plate made of two thin sheets of chrome-plated copper with a foil heater sandwiched between them; the external sides of the plate are roughened with transverse, square-cross-sectioned ribs. Results include flow schlieren visualizations and reconstruction of the local heat transfer coefficient distribution along the ribbed surface.**

***Keywords*—schlieren, natural convection, ribbed channel, water**

I. Introduction

The schlieren technique has long been an attractive diagnostic tool for the study of fluid flow fields. Since the schlieren effect is related to gradients of the refractive index, density/temperature variations in a fluid flow can be easily visualized by means of this optical method, basically requiring a white light source, an optical setup made of mirrors or lenses, a camera and a special filter to detect the light deflections in the observed field. A comprehensive and exhaustive description of the schlieren technique, including qualitative and quantitative applications, optical principles and devices to detect light deflections, is provided in the book by Settles [1].

Due to the simple relationship between the refractive index and the density of gases, the schlieren technique has been mainly employed for the investigation of flow and thermal fields using a gas as flowing medium [1]. Conversely, schlieren was not a popular method in the past to visualize liquid flows. Liquids usually induce strong light refractions and this limits the use of schlieren devices, which do not typically need or want high sensitivity, to phenomena characterized by very small changes in temperature or a very small width of the test section in the light beam direction. In addition, quantitative results can be gained if the refractive index variations with the liquid temperature and pressure are precisely known *a priori*.

The Authors of the present work were apparently the first to apply a quantitative schlieren technique to the study of heat transfer in liquid flows [2,3]; in particular, local heat transfer coefficients along a vertical plate in the presence of laminar, natural convective water flow have been determined. Their past experiments performed proved the validity of the experimental method and its applicability to the study of thermal fields not only in gases but even in transparent liquid flows.

The present work aims at gaining qualitative and quantitative visualization of natural convection in water channels having repeated ribs on the heat transfer surfaces. These surfaces are commonly encountered in several engineering applications (electronic equipment, solar collectors, passive heating of buildings, etc.). Moreover, there are situations (surfaces of buildings, electronic circuit boards) in which the roughness occurs naturally and is not added for the specific purpose of modifying heat transfer performance. Thus, understanding the thermal behaviour of these systems is essential for their correct design [4,5].

II. Background

The angular deflection of a light ray due to a density/temperature gradient in a fluid layer can be estimated from geometrical optics.

Let us consider a light ray, propagating along the *z*-axis of a Cartesian *x*-*y*-*z* coordinate system, which passes through a fluid layer, of depth *L*, bounded by two surfaces lying onto *x*-*y* parallel planes, as shown in Fig.1. The deflection angle of the light ray in the *y* direction as it reaches the *x*=*L* plane is given by

$$\alpha_y = \int_0^L \frac{1}{n}\frac{\partial n}{\partial y} dz \qquad (1)$$

where *n* is the refractive index of the fluid and the integration is performed over the entire length of the light ray in the fluid layer. Eq. (1) is derived under the assumption of very small angles of deflection.

Authors:

Marco Fossa,
Mario Misale,
Giovanni Tanda,
DIME, Università degli Studi di Genova,
Genova, Italy

If the phenomenon under study is two-dimensional, i.e. density/temperature of the fluid does not depend on *z*-coordinate, as the entering angle is zero, the angle at $z=L$ is

$$\alpha_y = \frac{L}{n_0}\frac{\partial n}{\partial y} \tag{2}$$

where the term $1/n$ within the integral has been assumed not to change greatly through the test section and set equal to $1/n_0$, n_0 being a reference value for the fluid refractive index. As the gradient of the refractive index with respect to the temperature is introduced, Eq.(2) becomes

$$\alpha_y = \frac{L}{n_0}\frac{\mathrm{d}n}{\mathrm{d}T}\frac{\partial T}{\partial y} \tag{3}$$

For gases, $\mathrm{d}n/\mathrm{d}T$ can be easily deduced by applying the Gladstone-Dale and the ideal gas laws to give $\mathrm{d}n/\mathrm{d}T = -K\,P/(R\,T^2)$, where K is the Gladstone-Dale constant, R is the ideal gas constant, P is the pressure and T is the absolute temperature. For liquids, $\mathrm{d}n/\mathrm{d}T$ has to be experimentally determined. In the case of water, Harvey et al. [6] reported the refractive index at different wavelength in the visible spectrum, versus pressure and temperature. A fitting of data, at the atmospheric pressure and averaged over the visible wavelength range, gave $n_0 = 1.335$ (at 20°C) and the following relationship of $\mathrm{d}n/\mathrm{d}T$ with T in the 15-40°C range

$$\mathrm{d}n/\mathrm{d}T = -1.1869 \times 10^{-5} - 4.4407 \times 10^{-6}\,T + 2.5 \times 10^{-8} T^2 \tag{4}$$

where the fluid temperature T is expressed in °C. It is worthy of note that averaging $\mathrm{d}n/\mathrm{d}T$ with the wavelength results in a 2% maximum deviation from Eq.(4) if any single wavelength in the visible spectrum is considered.

In the case of a water layer, enclosed by glass walls (plane and at uniform thickness) and surrounded by ambient air (at refractive index n_{air}), an additional angular deflection occurs according to Snell's law. If α'_y is the angle of the light ray as it emerges into the surrounding air after it has passed through the water layer, it follows that

$$\alpha'_y = \alpha_y \frac{n_0}{n_{air}} \tag{5}$$

where, due to the small values of the angles, $\sin\alpha'_y$ and $\sin\alpha_y$ have been replaced by α'_y and α_y, respectively, while (n_0/n_{air}) is the ratio between refractive indices of water and air at a standard condition (20°C, atmospheric pressure).

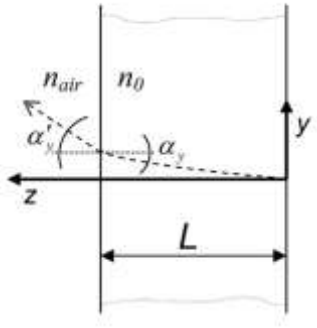

Figure 1. Deflection of a light ray due to optical disturbances in a fluid layer of depth L. Snell's law applies at the fluid/air interface if the fluid refractive index n_0 significantly differs from the air refractive index n_{air}

III. The Experiment

A. The Optical Setup

The Z-type schlieren arrangement used in the present experiment is shown in Fig.2. A noncoherent light beam coming from a 30μm-wide vertical slit source is collimated by the concave mirror M_1 to form parallel light rays crossing the test section, located inside a water chamber. Without inhomogeneities of the water refractive index in the test section, the parallel light rays, focused by the concave mirror M_2, converge to a thin vertical line on the primary focal plane, representing the primary image of the light source and called primary focal line. All rays are then projected onto the screen (image plane) where a real image of the test section is formed. When inhomogeneities are present in the test section, the light rays undergo angular deflections. All rays (deflected and non-deflected) are recombined on the screen, where a non-distorted image of the test section is still formed.

Regions of the test section that give rise to the same light angular deflection along the y direction can be identified by using a vertical filament (for instance a thin opaque strip or wire) in the primary focal plane of mirror M_2 (also called the *schlieren head*). On this plane, the deflected rays are shifted by a quantity Δ_y given by

$$\Delta_y = f_2\alpha'_y = f_2\alpha_y \frac{n_0}{n_{air}} \tag{6}$$

where f_2 is the distance between mirror M_2 and the primary focal line, n_{air} (=1.0003) is the refractive index of ambient (laboratory room) air and n_0 (=1.335) is the refractive index of water at a standard condition. It is useful to remind that α_y is the angular deflection, along the y direction, induced by thermal gradients in the water according to Eq.(3). In order to detect the light shifting Δ_y (and the related angular deflection), the focal filament is first placed in its reference position (position 1 in Fig.3). This position, for which the primary

focal line is completely intercepted by the filament, can be clearly identified since it corresponds, without inhomogeneities in the fluid, to a uniformly dark image on the screen. Then, moving the vertical filament in the focal plane, parallel to itself, allows one to measure the values of the light ray deflections in the whole optical field. For instance, when the focal filament is shifted from position 1 to position 2 (Fig.3) by a known quantity Δ_y, a shadow is formed on the image plane. This shadow defines the locus of the images of points deflecting the light by the same angle (termed curve of equal light deflection angle or, more simply, *iso-deflection* line). When deflections of light rays passing in the vicinity of the heated wall are of interest (in order to deduce the heat transfer coefficient), the focal filament has to be shifted until its shadow, projected onto the image plane, intercepts the vertical surface profile at the desired location.

This schlieren technique, called *focal filament method* by Vasil'ev [7], in special conditions allows a direct measurement of the local heat transfer coefficient. For this purpose, the local convective heat transfer coefficient is now introduced

$$h = -\frac{k_w}{(T_w - T_f)}\left(\frac{\partial T}{\partial y}\right)_w \qquad (7)$$

where $(\partial T/\partial y)_w$ is the fluid temperature gradient, in the direction y normal to the heated plate, evaluated at the wall, T_w is the wall temperature, k_w is the thermal conductivity of the fluid at the wall temperature and T_f is the fluid temperature.

From the combination of Eqs.(3), (5), (6) and (7), it follows that

$$h = -\frac{k_w}{(T_w - T_f)}\left(\frac{n_{air}\Delta_w}{f_2 L(\mathrm{d}n/\mathrm{d}T)_w}\right) \qquad (8)$$

where the subscript w denotes quantities to be evaluated at the wall. Therefore, assuming the water properties k and dn/dT as known, provided that T_w and T_f are independently measured, Eq.(8) states the direct relationship between the optical quantity Δ_w and the local heat transfer coefficient for a 2-D thermal field. In particular, Δ_w represents the shifting of the light ray passing in the vicinity of the heated wall and is detected by the schlieren apparatus according to the procedure illustrated in Fig.3.

A filter, operating according to the principles of the focal filament previously described, has been obtained by photographing a violet strip using a slide film. The slide produced in this manner, consisting of a 370μm-wide, transparent, violet band, was directly used as focal filament filter. As the filter is vertically mounted in the focal plane of mirror M_2, light rays deflected by the same angle pass through the violet band, and the corresponding points of the test section appear, in the image plane, coloured in violet. The width of the violet band was properly selected in order to minimize light diffraction effects and to provide a relatively high sensitivity of the technique. The use of a transparent colour band instead of an opaque band makes it easier to identify the correct location of the intersection between the iso-deflection line (appearing violet in the image plane) and the surface wall profile (appearing black in the image plane). To facilitate the description of successive steps, the violet band will be simply termed *focal filament*.

B. The Test Section

The description of the test section used in the experiments is facilitated by the schematic view presented in Fig.4. The thermally active component of the apparatus was a vertical plate (termed *heated plate*) made of two thin sheets of chrome-plated copper with a 0.5mm-thick electric foil heater sandwiched between them. The two copper sheets were sealed with a water-resistant cement to prevent any contact between the heater and the water. When electrical power was delivered to the heater, the heated plate was expected to attain a uniform surface temperature at the steady state owing to the high thermal conductivity of copper. The dimensions of the heated plate were the following: height H = 87 mm, length L = 48 mm, overall thickness t = 8 mm. Each side of the heated plate exposed to the water flow was roughened with five transverse, square-cross-sectioned ribs, made integral with the baseplate to guarantee the absence of contact resistance. The square ribs had a height e of 2.42 mm and were regularly spaced at intervals of P = 17.4 mm, resulting in a pitch-to-height ratio P/e =7.2.

Two parallel vertical walls, smooth and unheated, formed with the heated plate two adjacent, identical, and asymmetrically heated, channels. The spacing S between each unheated wall and the heated plate, set equal on both sides, was 17.4 mm, corresponding to a channel aspect ratio S/H equal to 0.2. The symmetrical arrangement of the heated plate/shrouding wall assembly permitted the optical measurements to be repeated on both sides and, owing to the symmetry, averaged at the same elevation, thus reducing the experimental error.

The heated and unheated walls were suspended, by using a supporting frame, inside a tank with inner dimensions 180x65x390 mm (width x length x height) filled with distilled water. Special care was taken in the design of the supporting frame to permit the correct positioning of the channel walls and to avoid flow obstructions in the vicinity of the channel openings. The tank was open on the top side to provide ambient pressure conditions at the air/water interface. The exit of the channel was situated 75 mm below the water surface and the entrance at 190 mm above the tank inner floor. The vertical sides of the tank normal to the light beam were made of 6mm-thick, high quality glasses so as to permit the schlieren measurements. The remaining sides and the bottom of the tank were made of 10mm-thick chrome-plated copper and finned on the ambient air side to facilitate the dissipation of the input power to the laboratory ambient air and to reduce, as much as possible, the thermal stratification in the fluid.

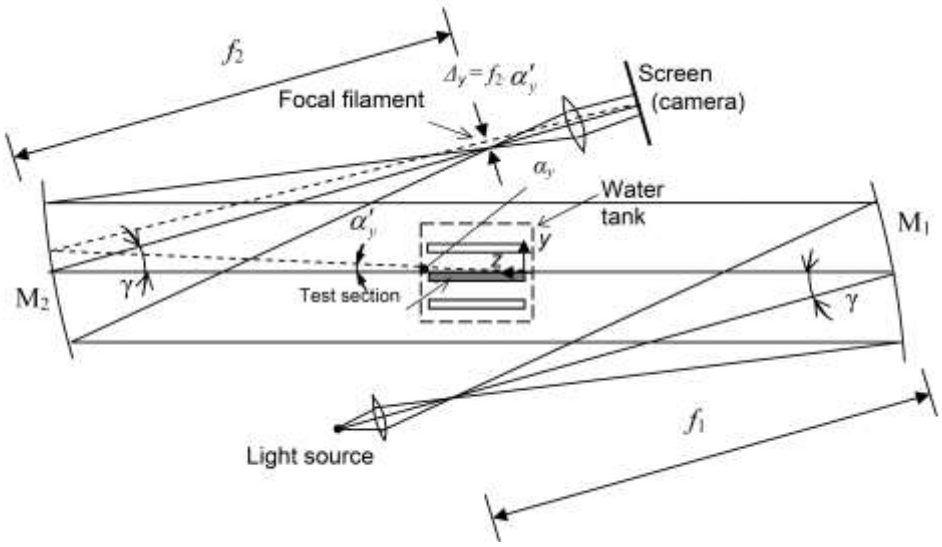

Figure 2. Schematic layout of the Z-shaped schlieren system (top view); M_1 and M_2 are 380 mm diameter concave mirrors (with focal lengths f_1 and f_2, respectively), α_y is the y-component of the light ray angular deflection within the test section, α'_y is the angular deflection of the light ray emerging into the ambient air, and Δ_y is the related shifting at the focal plane of mirror M_2.

The heated plate and the water tank were instrumented with 0.5-mm-dia sheathed thermocouples, calibrated to ± 0.05 K. Six thermocouples were placed into the heated plate at different locations through small diameter holes drilled into the material as close to the exposed surfaces as possible. The wall temperature T_w was obtained by averaging the readings of the six thermocouples embedded in the plate material. The fluid temperature T_f was measured by a thermocouple located at the inlet section of one of the two identical channels; an additional thermocouple, able to travel vertically within the tank and outside the channels, was used to check the presence of undesirable water fluid temperature stratification.

C. *The Experimental Uncertainty*

The uncertainty in the results (at the 95% confidence level) was evaluated by using a root-sum-square of the contributions made by the uncertainties in each of the individual measurements. The uncertainty in the local heat transfer coefficient h as expressed by Eq.(8) is generally sensitive to the errors associated with the temperature measurements, with the dn/dT relationship assumed for water, and with the schlieren Δ_w readings. The accuracy in schlieren Δ_w readings improves with increasing Δ_w, whose value was, for the present experiment, typically between 3 and 6 mm, with associated errors of less than 10%. As errors in the wall-to-fluid temperature difference and dn/dT relationship are accounted for, the uncertainty in h values falls into the 15-18% range.

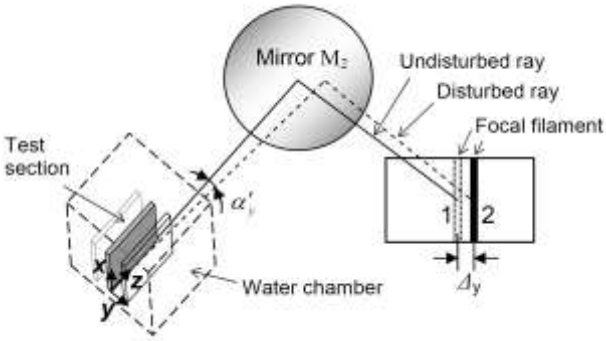

Figure 3. Measurement of the shifting Δ_y of the deflected ray in the focal plane of schlieren mirror M_2 by means of the focal filament, moved from position 1 to position 2.

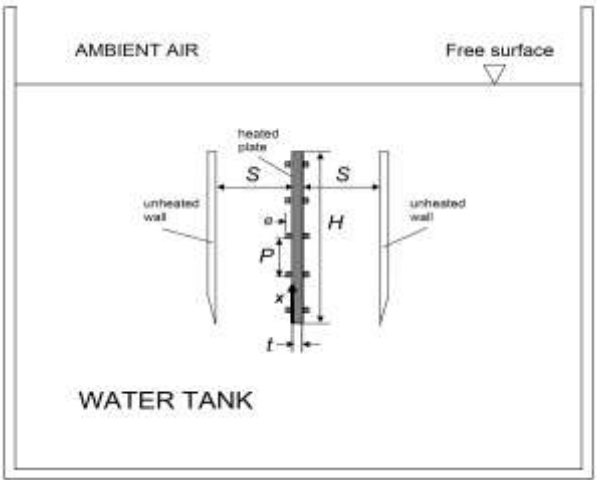

Figure 4. Schematic layout of the vertical ribbed channels inside the water tank. Drawing not to scale.

IV. The Results

The aim of the present work was to apply the focal filament schlieren method to measure the local heat transfer coefficient for the buoyancy-induced water flow in an asymmetrically heated, ribbed vertical channel having an aspect ratio *S/H* equal to 0.2. Heat transfer experiments were performed by keeping the input power, delivered to the heated plate, in the 3 - 4 W range, giving a wall-to-fluid temperature difference of 1.4 to 1.8 K. Depending on the laboratory room temperature, steady-state values of T_w and T_f were in the 19-21°C and 17-20°C ranges, respectively. These experimental conditions were selected in order to achieve the best compromise between schlieren sensitivity and measurement accuracy.

Typical examples of photographs taken by the schlieren apparatus using the focal filament method are reported in Fig. 5. As explained previously, the thin line visible in the ribbed channel identifies the zones of fluid that give rise to a known light ray angular deflection (related to the displacement of the focal filament from its original reference position). In order to detect angular deflections of rays passing in the vicinity of the heated wall, the focal filament has to be moved (as shown in the sequence of pictures displayed in Fig.5) until the corresponding iso-deflection line generated in the image plane intercepts the wall profile at a given point.

Figure 6 shows the distribution of the local heat transfer coefficient *h* along the heated plate measured for a wall-to-fluid temperature difference of 1.5 K. Different symbols for the inter-rib and the rib (at the center of each vertical side) regions have been adopted. For comparison purposes, the *h*-distribution obtained in [2] for a smooth vertical channel, by using the same fluid, experimental technique, aspect ratio and wall-to-fluid temperature difference, is reported. Inspection of the figure reveals that along the inter-rib regions heat transfer coefficient distribution is characterized by low values close to the ribs, due to the presence of fluid stagnation zones just upstream and downstream of each rib. The space between ribs is sufficient for the main flow to wash the inter-rib surfaces before being deflected by the next rib downstream; this explains the presence of heat transfer coefficient peaks approximately at the midpoint of each inter-rib region. The developing thermal field is responsible for the progressive reduction of *h* values registered at points separated by an elevation equal to the rib pitch. Relatively high heat transfer coefficients are found on the vertical sides of ribs since they are washed by cool water flow. The heat transfer performance of the ribbed surface is typically lower than that obtained for the smooth surface, with the exception of points located on the ribs close to the channel exit.

Figure 5. Schlieren images recorded with the focal filament progressively moved from its reference position in order to show the images of points of the optical field deflecting the light by the same known amount.

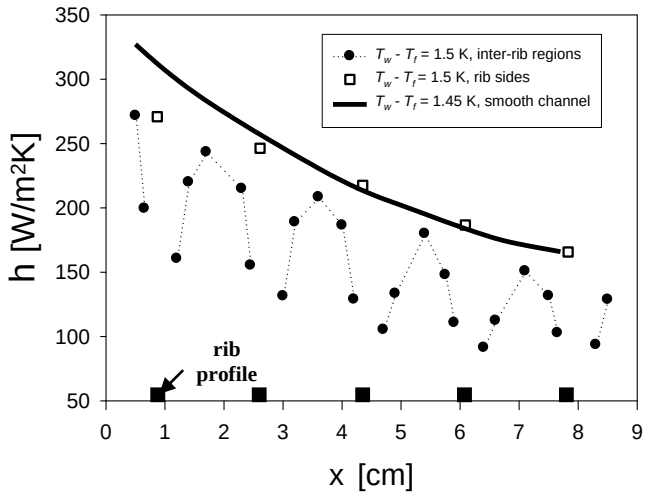

Figure 6. Local heat transfer coefficients along the heated plate with ribs (symbols) and without ribs (solid line).

References

[1] G.S. Settles, Schlieren and Shadowgraph Techniques, Springer, 2001.

[2] G. Tanda, M. Misale, and M.Fossa, "Heat transfer measurements in water using a schlieren technique", Int. J. Heat Mass Transfer, vol.71, pp. 451- 458, 2014.

[3] M. Misale, M. Fossa, and G. Tanda, "Investigation of free convection in a vertical water channel", Exp. Thermal Fluid Science, vol. 59, pp. 252-257, 2014.

[4] S.H. Bhavnani and A.E. Bergles, "Effect of surface geometry and orientation on laminar natural convection heat transfer from a vertical flat plate with transverse roughness elements", Int. J. Heat Mass Transfer, vol.33, pp. 965-981, 1990.

[5] G.Tanda, "Natural convection heat transfer in vertical channels with and without transverse square ribs", Int. J. Heat Mass Transfer, vol.40, pp. 2173-2185, 1997.

[6] A.H. Harvey, J.S.Gallagher, and J.M.H. Levelt Sengers, "Revised formulation for the refractive index of water and steam as a function of wavelength, temperature and density", J. Physical Chemical Ref. Data, vol.27, pp.761-774, 1998.

[7] L.A. Vasil'ev , Schlieren Methods, Keter Inc., 1971.